PROCEEDINGS OF SCIENCE

Pre-supernova models at very low metallicity

Raphael Hirschi*
Dept. of physics and Astronomy, University of Basel, Klingelbergstr. 82, CH-4056 Basel
E-mail: Raphael.Hirschi@unibas.ch

A series of fast rotating models at very low metallicity ($Z = 10^{-8}$) was computed in order to explain the surface abundances observed at the surface of CEMP stars, in particular for nitrogen. The main results are the following:

- Strong mixing occurs during He–burning and leads to important primary nitrogen production.
- Important mass loss takes place in the RSG stage for the most massive models. The 85 $M_{\odot}$ model loses about three quarter of its initial mass, becomes a WO star and could produce a GRB.
- The CNO elements of HE1327-2326 could have been produced in massive rotating stars and ejected by their stellar winds.

International Symposium on Nuclear Astrophysics — Nuclei in the Cosmos — IX
June 25-30 2006
CERN, Geneva, Switzerland

*Speaker.

PoS(NIC-IX)116

1. Introduction

Precise measurements of surface abundances of extremely metal poor (EMP) stars have recently been obtained [2, 21, 15]. These provide new constraints for stellar evolution models (see [3, 7, 19]). The most striking constraint is the need for primary ^{14}N production in very low metallicity massive stars. About one quarter of EMP stars are carbon rich (C-rich EMP, CEMP stars). Ryan et al [20] propose a classification for these CEMP stars. They find two categories: about three quarter are main s–process enriched (Ba-rich) CEMP stars and one quarter are enriched with a weak component of s–process (Ba-normal). The two most metal poor stars known to date, HE1327-2326 [8, 1] and HE 0107-5240 [5] are both CEMP stars. These stars are thought to have been enriched by only one to several stars and the yields of the models can therefore be compared to their observed abundances without the filter of a galactic chemical evolution model.

The evolution of very low metallicity or metal free stars is not a new subject (see for example [4, 6]). The observations cited above have however greatly increased the interest in very metal poor stars. There are many recent works studying the evolution of metal free (or almost) massive [10, 16, 23, 17], intermediate mass [22] and low mass [24] stars. In this work pre-supernova evolution models of rotating single stars were computed at a metallicity, $Z = 10^{-8}$ to study the impact of rotation in the evolution of very low metallicity stars.

2. Computer model & calculation

The computer model used here is the same as the one described in [12]. Convective stability is determined by the Schwarzschild criterion. Overshooting is only considered for H– and He–burning cores with an overshooting parameter, $\alpha_{\rm over}$, of 0.1 H_P. Models were computed at Z=10^{-8} with initial masses of 20, 40, 60 and 85 $M_\odot$ and initial rotational velocities of 600, 700, 800 and 800 km s^{-1} respectively. At first sight, these velocities appear to be very high but their corresponding total angular momentum is similar to the one contained in solar metallicity stars with rotational velocities of 300 km s^{-1}. The evolution of the models was followed until core Si–burning except for the 60 $M_\odot$, which was followed until neon burning. The yields of these models were calculated in the same way as in [14]. The (pre–)SN yields were calculated without taking into account the explosive nucleosynthesis. We therefore only present yields of light elements, which are not significantly affected by the subsequent evolution.

3. Evolution of the structure

The evolution of the structure of the models is shown in Fig. 1. A strong mixing takes place during He–burning. Primary carbon and oxygen are mixed outside of the convective core into the H–burning shell. Once the enrichment is strong enough, the H–burning shell is boosted. The H–burning shell then becomes convective. In response to the shell boost, the core expands and the convective core mass decreases. At the end of He–burning, the CO core is smaller in mass than in non–rotating models (see [11]). The yield of ^{16}O being closely correlated with the mass of the CO core, it is therefore reduced due to the strong mixing. At the same time the carbon yield is slightly increased. It is interesting to note that the shell H–burning boost occurs in all the different

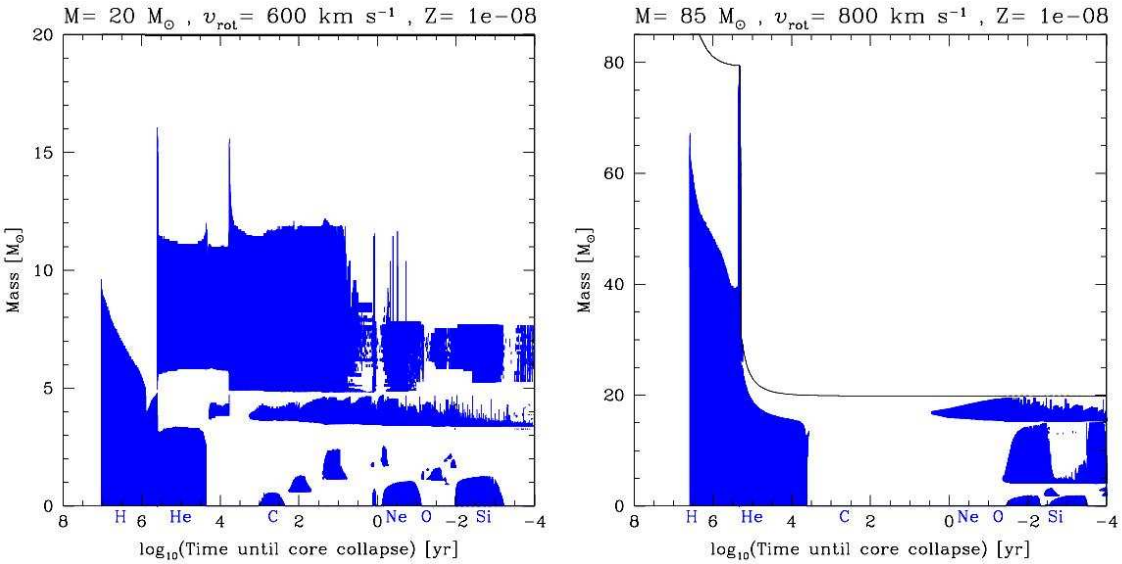

Figure 1: Stellar structure (Kippenhahn) diagrams, which show the evolution of the structure as a function of the time left until the core collapse for the 20 $M_\odot$ (*left*) and 85 $M_\odot$ (*right*). The coloured zone correspond to the convective zones and the symbols of the burning stages are given below the time axis.

initial mass models at $Z = 10^{-8}$. This means that the strong mixing could be an explanation for the possible high [C/O] ratio observed in the most metal poor halo stars (see Fig. 14 in [21]).

The 85 $M_\odot$ model becomes a WO type (see Fig. 2) WR star. SNe of type Ib,c are therefore expected to ensue from the death of single massive stars at very low metallicities. The core of the 85 $M_\odot$ model retains enough angular momentum to produce a GRB via the collapsar model (see [26, 25, 13] for more details on GRB progenitors).

4. Wind and pre–SN composition and comparison with CEMP stars

The CNO abundances of HE1327-2326 could be explained with the following scenario. A first generation of stars (PopIII) pollutes the interstellar medium to very low metallicities ([Fe/H]$\sim$-6). Then a PopII.5 star like the 40 $M_\odot$ model calculated here pollutes (mainly through its wind) again the interstellar medium out of which HE1327-2326 forms. In this scenario, the CNO abundances are well reproduced, in particular that of nitrogen, which according the new values for a subgiant from [9] is 0.9 dex higher in [X/Fe] than oxygen. This is shown in Fig. 3 where the new abundances are represented by the red stars and the best fit is obtained by diluting the composition of the wind of the 40 $M_\odot$ model by a factor 600. On the right side, one sees that when the SN contribution is added, the [X/Fe] ratio is usually lower for nitrogen than for oxygen.

References

[1] Aoki, W., Frebel, A., Christlieb, N., et al. 2006, ApJ, 639, 897

[2] Cayrel, R., Depagne, E., Spite, M., et al. 2004, A&A, 416, 1117

[3] Chiappini, C., Matteucci, F., & Ballero, S. K. 2005, A&A, 437, 429

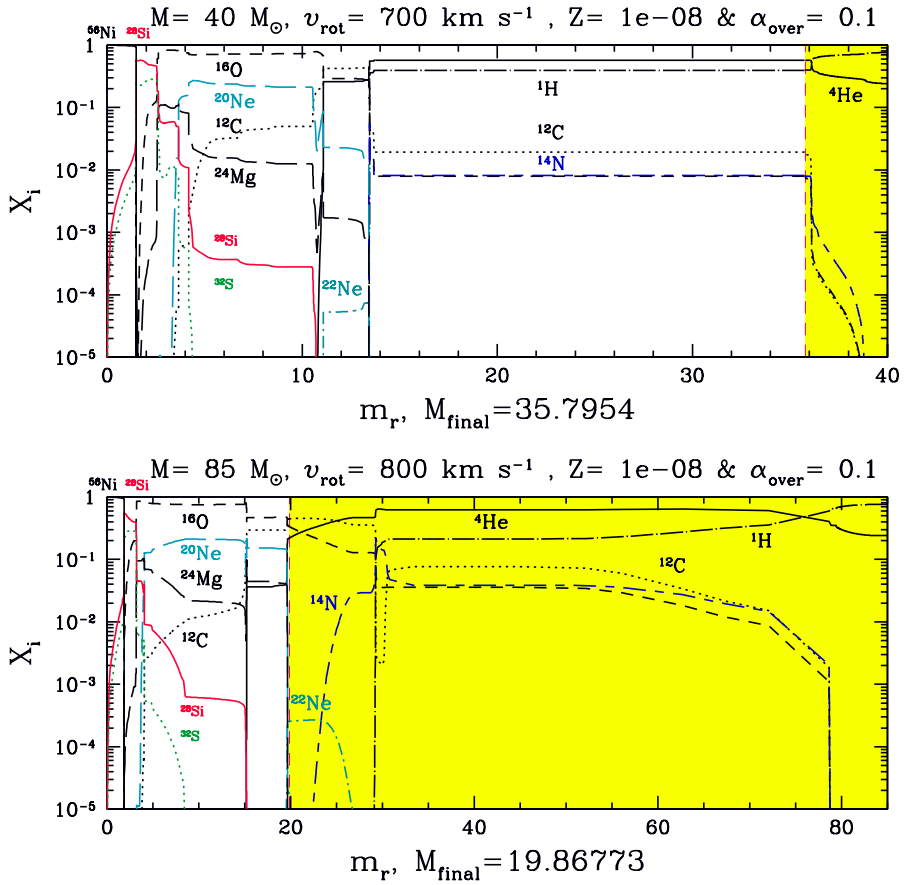

Figure 2: Abundance profiles for the 40 $M_\odot$ (*top*) and 85 $M_\odot$ (*bottom*) models. The pre–SN profiles and wind (yellow shaded area) profiles are separated by a red dashed line located at the pre–SN total mass ($M_{\rm final}$), given below each plot.

[4] Chiosi, C. 1983, Memorie della Societa Astronomica Italiana, 54, 251

[5] Christlieb, N., Gustafsson, B., Korn, A. J., et al. 2004, ApJ, 603, 708

[6] El Eid, M. F., Fricke, K. J., & Ober, W. W. 1983, A&A, 119, 54

[7] François, P., Matteucci, F., Cayrel, R., et al. 2004, A&A, 421, 613

[8] Frebel, A., Aoki, W., Christlieb, N., et al. 2005, Nature, 434, 871

[9] Frebel, A., Christlieb, N., Norris, J. E., Aoki, W., & Asplund, M. 2006, ApJ, 638, L17

[10] Heger, A. & Woosley, S. E. 2002, ApJ, 567, 532

[11] Hirschi, R. 2006, A&A submitted

[12] Hirschi, R., Meynet, G., & Maeder, A. 2004, A&A, 425, 649

[13] Hirschi, R., Meynet, G., & Maeder, A. 2005a, A&A, 443, 581

[14] Hirschi, R., Meynet, G., & Maeder, A. 2005b, A&A, 433, 1013

[15] Israelian, G., Ecuvillon, A., Rebolo, R., et al. 2004, A&A, 421, 649

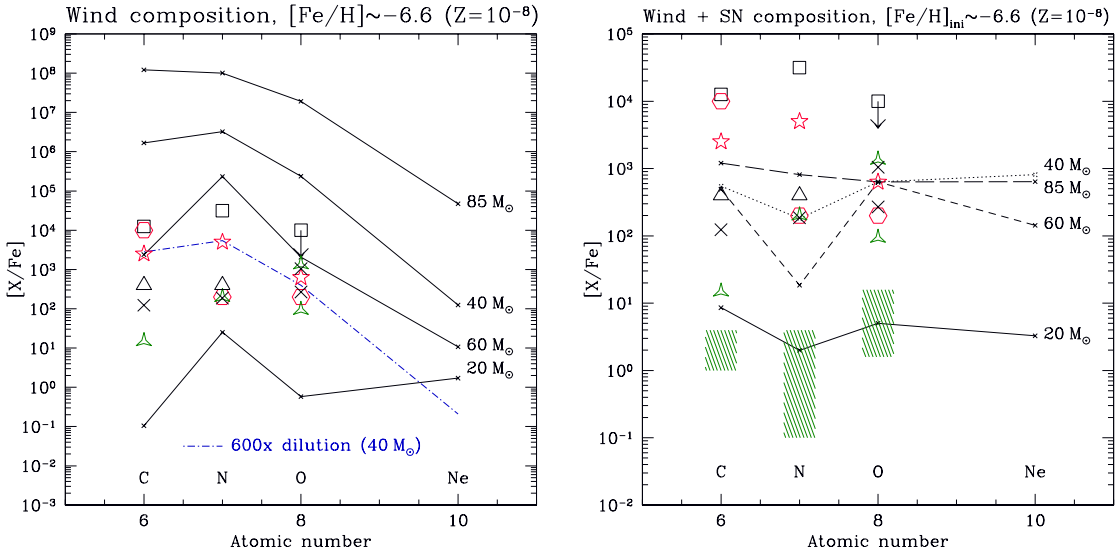

Figure 3: Composition in [X/Fe] of the stellar wind (*left*) and the sum of the wind and SN ejecta (*right*) for the $Z = 10^{-8}$ models. The lines represent predictions from the models. The *empty triangles* [18], and *squares* [8], [Fe/H]$\simeq -5.4$ correspond to non-evolved CEMP stars. The new (3D/NLTE corrected) estimates for HE1327-2326 from [9] are represented by the *red stars*. On the right, wind+SN ejecta is compared to the normal EMP stars [2, 21] for the 20 $M_\odot$ model (green hatched area) and again to the CEMP stars for the more massive models. For this purpose, the value [O/Fe] is chosen to fall in the middle of the observed range (20 $M_\odot$: [O/Fe]=0.7 and $M > 20 M_\odot$: [O/Fe]=2.8). The other symbols correspond to the abundances measured at the surface of giant CEMP stars.

[16] Limongi, M. & Chieffi, A. 2005, astro-ph/0507340, IAU228

[17] Meynet, G., Ekström, S., & Maeder, A. 2006, A&A, 447, 623

[18] Plez, B. & Cohen, J. G. 2005, A&A, 434, 1117

[19] Prantzos, N. 2005, Nuclear Physics A, 758, 249

[20] Ryan, S. G., Aoki, W., Norris, J. E., & Beers, T. C. 2005, ApJ, 635, 349

[21] Spite, M., Cayrel, R., Plez, B., et al. 2005, A&A, 430, 655

[22] Suda, T., Aikawa, M., Machida, M. N., Fujimoto, M. Y., & Iben, I. J. 2004, ApJ, 611, 476

[23] Umeda, H. & Nomoto, K. 2005, ApJ, 619, 427

[24] Weiss, A., Schlattl, H., Salaris, M., & Cassisi, S. 2004, A&A, 422, 217

[25] Woosley, S. E. & Heger, A. 2006, ApJ, 637, 914

[26] Yoon, S.-C. & Langer, N. 2005, A&A, 443, 643